Chemistry of Metals and Alloys

Chem. Met. Alloys 18 (2025) 36-43
Ivan Franko National University of Lviv
https://publications.lnu.edu.ua/chemetal

MAX phases in the system Ti–Al–C: synthesis and hardness

Anastasiia BRODA[1]*, Roman GLADYSHEVSKII[1]

[1] *Department of Inorganic Chemistry, Ivan Franko National University of Lviv, Kyryla i Mefodiya St. 6, 79005 Lviv, Ukraine*
* *Corresponding author. Tel.: +380-32-2600388; e-mail: Anastasiia.Broda.hmh@lnu.edu.ua*

Received November 28, 2025; accepted December 23, 2025
https://doi.org/10.30970/cma18.0454

The MAX phases Ti_2AlC and Ti_3AlC_2 were synthesized by spark plasma sintering at different temperatures. Differential thermal analysis showed that the temperatures of maximum formation for the two phases differ by only ~20°C. Optimal synthesis temperatures were found to be 1300°C for Ti_2AlC and 1350°C for Ti_3AlC_2. X-ray diffraction revealed cell parameters in agreement with literature data and the absence of homogeneity regions. The synthesized materials exhibited low densities, 4.09 and 4.15 g·cm^{-3}, respectively, and Vickers hardness values of 3.4-6.0 GPa for Ti_2AlC and 3.2-3.9 GPa for Ti_3AlC_2.

MAX phases / Spark Plasma Sintering / X-ray powder diffraction / Crystal structure

Introduction

MAX phases are well-known for their unique combination of properties and their versatility. As of today the family contains more than 150 different representatives. Wolfgang Jeitschko and Hans Nowotny discovered more than 100 carbides and nitrides, among which MAX phases in the Ti–Al–C system [1,2]. The Ti–Al–C system contains three compounds that are part of the MAX phases: Ti_2AlC [3,4], Ti_3AlC_2 [3,5-7], and $Ti_5Al_2C_3$ [3,8-10].

The basic MAX phases have hexagonal crystal structures with space group $P6_3/mmc$ and can be described by the general formula $M_{n+x}AX_n$, where M corresponds to a transition metal, A is an element of groups IIIA or IVA, X is C and/or N, and n is equal to 1, 2 or 3 [1]. The crystal structures of Ti_2AlC and Ti_3AlC_2 have been refined on diffraction data from polycrystalline samples, using X-ray [4,5], electron [7] or neutron radiation [3,6].

As noted above, the MAX phases are interesting for their properties. Most of them are electrically and thermally conductive, easily machinable, ductile with a high stiffness-to-hardness ratio, resistant to thermal shocks and chemical attacks, and maintain their strength at high temperatures [11]. Due to the attractive properties, not only ternary systems but also quaternary systems are being studied. Much attention is also paid to the methods of synthesis. The most commonly used methods are liquid/solid state reactions: spark plasma sintering (SPS), self-propagating high-temperature synthesis, hot pressing (HP), hot isostatic pressing (HIP), pressure-less synthesis, and microwave-supported preparation [1,10,12-16]. Interestingly, many synthetic methods have been employed, but it has not yet been possible to obtain a pure sample.

Experimental

Various methods and reagents were employed to find optimal synthesis conditions. A total of six samples with different nominal compositions were prepared: $Ti_{50}Al_{25}C_{25}$, $Ti_{53}Al_{25}C_{22}$, $Ti_{53}Al_{34}C_{13}$, $Ti_{50}Al_{27}C_{23}$, $Ti_{50}Al_{29}C_{21}$, and $Ti_{50}Al_{19}C_{31}$. Except for the sample $Ti_{50}Al_{25}C_{25}$, which was synthesized from a mixture of binary TiAl and TiC at a ratio of 1:1, the samples were prepared from a mixture of pure metal powders. Powders of Ti and Al with a purity of 99.999 wt.% and carbon (spectrographic, rods, purity ≥99.9995 wt.%) were ground, sieved through an 80 μm sieve, and mixed using ball milling. TiC powder with a purity of 99.995 wt.% and TiAl synthesized by arc-melting in a purified Ar atmosphere, were used for the preparation of $Ti_{50}Al_{25}C_{25}$.

The samples were synthesized by spark plasma sintering, SPS (Dr. Sinter, spark plasma sintering system, Sumitomo Coal Mining Co., Ltd.). The powder mixtures were placed in graphite molds between graphite punches (diameter 10 mm). Graphite

foil was used to prevent the mold from reacting with the sample. During the synthesis process, temperature and time were varied, maintaining a constant uniaxial pressure of 65 MPa. The maximal temperature T_{max} was found to be 1100°C for the samples $Ti_{53}Al_{25}C_{22}$ and $Ti_{53}Al_{34}C_{13}$, 1300°C for the samples $Ti_{50}Al_{27}C_{23}$ and $Ti_{50}Al_{29}C_{21}$, and 1350°C for the sample $Ti_{50}Al_{19}C_{31}$. To avoid losses, it was necessary to add excess aluminum to the initial mixture, as the sample might react with the foil and the mold. The temperature was monitored with a pyrometer. The synthesis was carried out under vacuum in steps to avoid losses. The temperature profile is shown in Fig. 1. After sintering, the samples $Ti_{53}Al_{25}C_{22}$ and $Ti_{53}Al_{34}C_{13}$ were ground, pressed into tablets, placed in corundum crucibles and sealed in glass ampoules. Annealing was carried out at 1070°C for 110 h and was followed by slow cooling to room temperature.

Differential thermal analysis (DTA) was performed using a NETZSCH DSC 404 C device under Ar atmosphere in a graphite crucible in a temperature range from room temperature to 1450°C or 1550°C with a heating rate of 10 K/min.

The crystal structures of the compounds were established by X-ray powder diffraction. Data for polycrystalline samples were collected on an Image Plate Guinier Huber G670 Camera (Cu $K\alpha_1$ radiation, $\lambda = 1.540562$ Å). The structural parameters were refined by the Rietveld method [17], using WinCSD software [18]. The structure drawings were made with the program ATOMS [19].

The microstructures of the samples and local chemical compositions were analyzed with a scanning electron microscope SEM Philips XL30 and Cameca SX100 Electron Microprobe, by standard-based wavelength-dispersive X-ray spectroscopy (WDXS) for the samples $Ti_{53}AL_{25}C_{22}$ and $Ti_{53}Al_{34}C_{13}$ and by energy-dispersive X-ray spectroscopy (EDXS) for the samples $Ti_{50}Al_{27}C_{23}$, $Ti_{50}Al_{29}C_{21}$ and $Ti_{50}Al_{19}C_{31}$.

The density of the samples was measured by hydrostatic weighing using a YDK 01 LP determination kit with LA/LP balances with a readability of 1 mg. Hardness was measured by a Vickers microhardness tester (0.005N÷4N) under different loads: 100 g, 300 g, and 400 g (samples $Ti_{50}Al_{27}C_{23}$, $Ti_{50}Al_{29}C_{21}$) using an optical microscope, or by a Novotest TS-MKV1 tester ($Ti_{50}Al_{19}C_{31}$). The measurements were made on sufficiently large areas including MAX phase grains.

Results and discussion

The DTA graph for the starting mixture $Ti_{50}Al_{25}C_{25}$ shows three exothermic peaks at 665(10)°C, 1411(10)°C, and 1420(10)°C (Fig. 2*a*). After the reaction, the PXRD pattern revealed, beside the educts, the presence of Ti_3AlC_2, TiC, $TiAl_3$, and minor amounts of Ti_2AlC (Fig. 3*a*). We believe that Al melts and reacts with Ti to form a binary compound at 665°C. The maximum amount of Ti_2AlC was present at 1411°C and the compound decomposed into Ti_3AlC_2 and $TiAl_3$ at 1420°C. Unfortunately, due to the small temperature difference, it was not possible to verify this theory. For comparison, a DTA analysis was performed on a 1:1 mixture of the binary compounds TiAl and TiC. As in the previous analysis, two peaks appeared on the DTA curve, but they were endothermic (Fig. 2*b*). We believe that the peak at 1436(10)°C is associated with the compound Ti_2AlC and the peak at 1440(10)°C with the compound Ti_3AlC_2. The diffraction diagram clearly shows the presence of these phases (Fig. 3*b*).

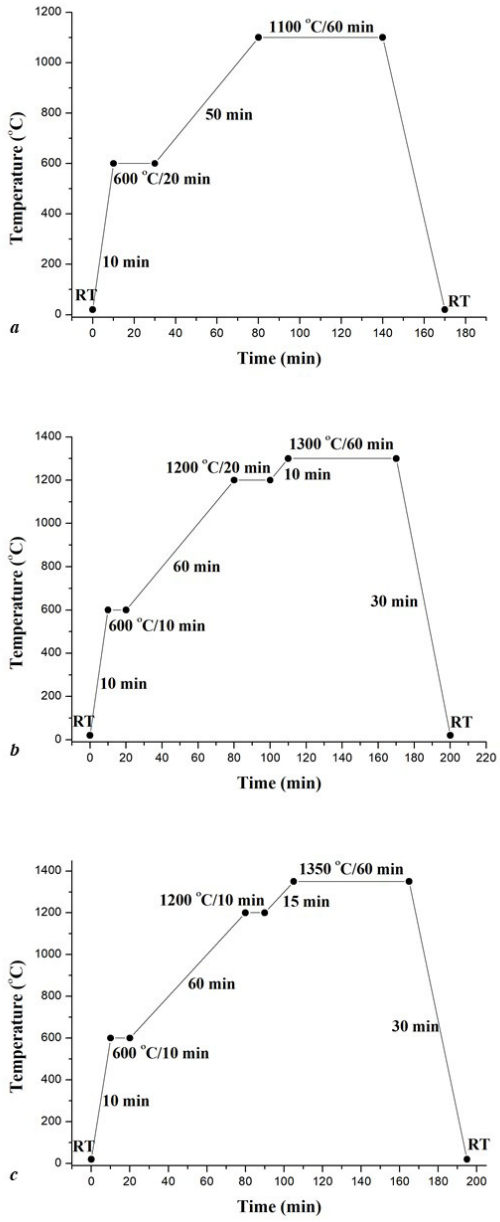


Fig. 1 Temperature profile for samples using SPS: (*a*) $Ti_{53}Al_{25}C_{22}$ and $Ti_{53}Al_{34}C_{13}$; (*b*) $Ti_{50}Al_{27}C_{23}$ and $Ti_{50}Al_{29}C_{21}$; (*c*) $Ti_{50}Al_{19}C_{31}$.

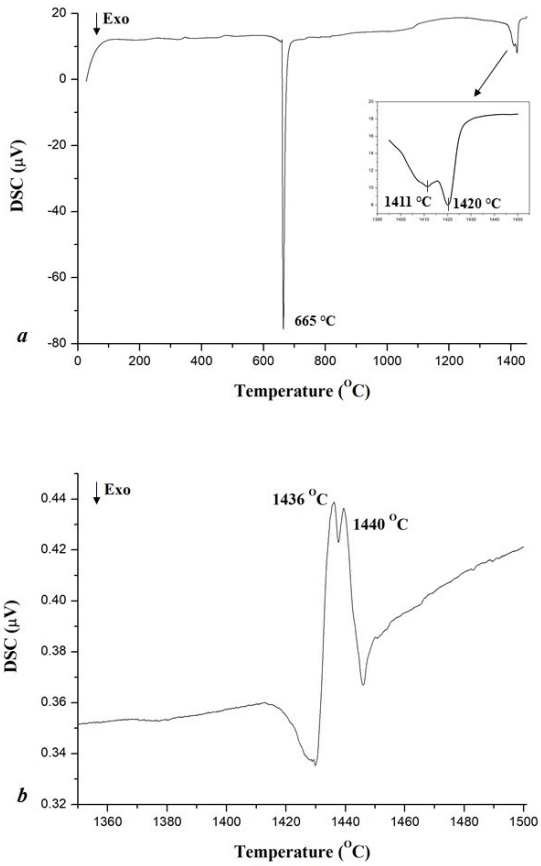


Fig. 2 DTA signal by heating of starting powder mixture of (*a*) $Ti_{50}Si_{25}C_{25}$ and (*b*) TiAl:TiC.

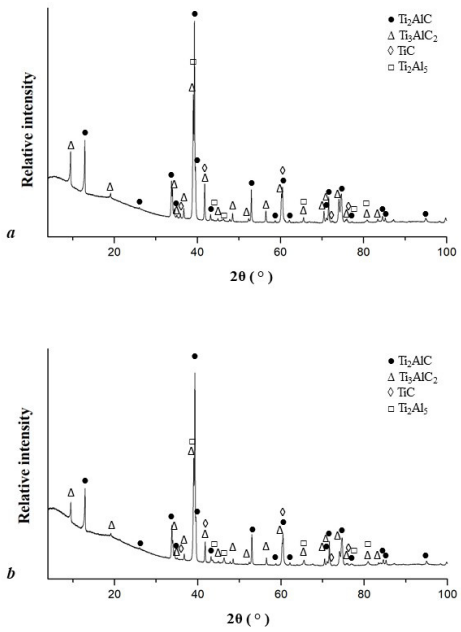


Fig. 3 Powder X-ray diffraction patterns of the reaction mixture (*a*) $Ti_{50}Si_{25}C_{25}$ after heating to 1450°C and (*b*) TiAl:TiC after heating to 1550°C.

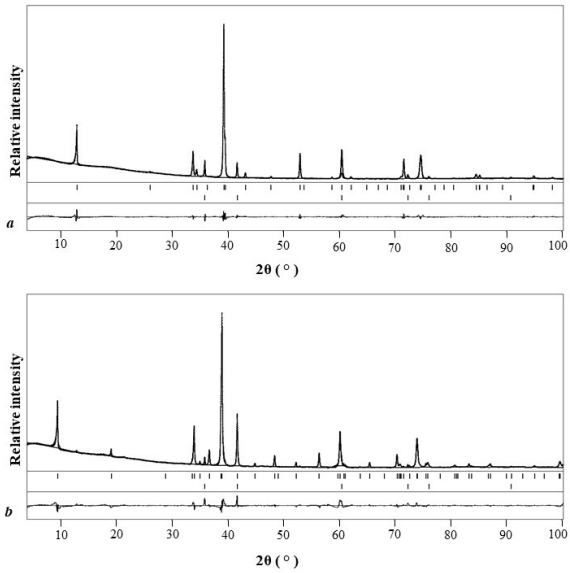


Fig. 4 Powder X-ray diffraction pattern of the sample after SPS preparation: (*a*) $Ti_{50}Al_{27}C_{23}$ (first line – Ti_2AlC; second line – TiC); (*b*) $Ti_{50}Al_{19}C_{31}$ (first line – Ti_3AlC_2; second line – TiC).

The PXRD patterns showed that the samples were not single-phase. The phase analysis revealed that the highest concentration of Ti_2AlC (211 phase) was in the sample $Ti_{50}Al_{27}C_{23}$, while the sample $Ti_{50}Al_{19}C_{31}$ contained the highest level of Ti_3AlC_2 (Table 1, Fig. 4). In addition to the primary phase the samples contained the binary compound TiC.

After having analyzed all the samples, we conclude that, for a synthesis using the SPS method, it is preferable to start from a mixture of pure metals. To obtain a maximum amount of 211 phase, it is necessary to prepare a starting mixture with more Al and less C (near 2 at.%) since the sample reacts with the graphite foil, and aluminum may be lost during the synthesis. Similar conditions should be fulfilled to obtain a maximum amount of 312 phase. To avoid the formation of the 211 phase, the temperature should be higher than 1350°C. At temperatures 1200-1300°C, it is possible to obtain a sample with two phases, or only the 211 phase. This compound can also be obtained at lower temperatures, around 1100°C, but after sintering in an SPS installation, the samples must be annealed at 1100°C. The samples $Ti_{53}Al_{25}C_{22}$ and $Ti_{53}Al_{34}C_{13}$ were annealed at 1070°C, because it was the highest achievable temperature. The diffractograms revealed that the samples were not single-phase, however, the annealing had increased the amount of Ti_2AlC to approximately 93(2) wt.% for the sample $Ti_{53}Al_{25}C_{22}$ and 95(3) wt.% for the sample $Ti_{53}Al_{34}C_{13}$. The secondary phases in the sample $Ti_{53}Al_{25}C_{22}$ were Ti_3Al (5.8(6) wt.%) and trace amounts of TiC (1.6(7) wt.%). The only secondary phase detected in the sample $Ti_{53}Al_{34}C_{13}$ was TiAl (5.0(9) wt.%).

Table 1 Experimental details and crystallographic data for the samples $Ti_{50}Al_{27}C_{23}$ and $Ti_{50}Al_{19}C_{31}$.

Sample	$Ti_{50}Al_{27}C_{23}$		$Ti_{50}Al_{19}C_{31}$	
Phase	Ti_2AlC	TiC	Ti_3AlC_2	TiC
Content, wt.%	89.4(4)	10.6(4)	95.1(5)	4.9(2)
Structure type	Cr_2AlC	NaCl	Ti_3SiC_2	NaCl
Space group	$P6_3/mmc$	$Fm\text{-}3m$	$P6_3/mmc$	$Fm\text{-}3m$
Pearson symbol	$hP8$	$cF8$	$hP12$	$cF8$
Cell parameters: a, Å	3.05688(6)	4.3242(1)	3.07027(8)	4.3249(2)
c, Å	13.6472(3)	–	18.5274(6)	–
Cell volume V, Å^3	110.442(4)	80.858(4)	151.252(7)	80.897(6)
Formula units per cell Z	2	4	2	4
Density D_X, g·cm^{-3}	4.055	4.923	4.277	4.921
Scale factor S_F	0.71		1.23	
Texture parameter G, direction	0.995(2), [001]	–	1.079(2), [001]	–
R_B	0.0360	0.0475	0.0596	0.0871
Number of reflections	30	5	40	5
FWHM parameters U, V, W	0.218(8), -0.140(7), 0.060(2)		0.33(1), -0.29(1), 0.084(2)	
Mixing parameter η	0.662(6)		0.825(7)	
Asymmetry parameter C_M	-0.204(4)		-0.131(3)	
Number of refined parameters	16		17	
Reliability factors: R_p, R_{wp}	0.0205, 0.0333		0.0236, 0.0386	

Table 2 Cell parameters of the compounds Ti_2AlC and Ti_3AlC_2 (this work and literature data).

Ti_2AlC			Ti_3AlC_2		
Sample/[Ref.]	Cell parameters, Å		Sample/[Ref.]	Cell parameters, Å	
	a	c		a	c
$Ti_{50}Al_{25}C_{25}$	3.0593(4)	13.660(2)	$Ti_{50}Al_{25}C_{25}$	3.0717(3)	18.558(2)
$Ti_{53}Al_{25}C_{22}$	3.0525(2)	13.6372(7)	$Ti_{50}Al_{19}C_{31}$	3.07027(8)	18.5274(6)
$Ti_{53}Al_{34}C_{13}$	3.0406(3)	13.6297(9)	[5]	3.0753	18.578
$Ti_{50}Al_{27}C_{23}$	3.05688(6)	13.6472(3)	[6]	3.073	18.557
$Ti_{50}Al_{29}C_{21}$	3.0551(2)	13.6413(6)	[3][a]	3.0642	18.5172
[4]	3.0502	13.6469	[3][a]	3.0667	18.5331
[3][a]	3.0566	13.6551	[3][a]	3.0689	18.5483
[3][a]	3.0591	13.6669	[3][a]	3.0711	18.5617
[3][a]	3.0614	13.6777	[3][a]	3.0736	18.5803
[3][a]	3.0635	13.6879	[3][a]	3.0763	18.5991
[3][a]	3.0663	13.7006	[3][a]	3.0791	18.6184
[3][a]	3.0692	13.7145	[3][a]	3.0821	18.638
[3][a]	3.0721	13.728	[3][a]	3.0852	18.6587
[3][a]	3.0751	13.7431	[3][a]	3.0882	18.6811
[3][a]	3.0782	13.7581	[7]	3.05	19.28
[3][a]	3.0813	13.7743			

[a] neutron diffraction data collected at 100, 200, 300, 400, 500, 600, 700, 800, 900, and 1000°C

Based on a comparison of the cell parameters of the compounds Ti_2AlC and Ti_3AlC_2 synthesized in this work and literature data, it appears that none of the compounds has a significant homogeneity range (Table 2).

In order to confirm the compositions of the title phases, metallographic analyses were carried out. In agreement with the PXRD data, the WDXS analysis showed that the samples $Ti_{53}Al_{25}C_{22}$ and $Ti_{53}Al_{34}C_{13}$ contained two phases (Fig. 5). For the sample $Ti_{53}Al_{25}C_{22}$ the first one (dark grey regions in the Fig. 5*a*) has an almost ideal Ti_2AlC composition, $Ti_{49(2)}Al_{24(1)}C_{27(2)}$, from WDXS. The second phase has the composition $Ti_{60(1)}Al_{33(6)}C_{7(4)}$ (gray in Fig. 5*a*). A similar situation occurs for the sample $Ti_{53}Al_{34}C_{13}$. The dark gray regions have the composition $Ti_{52(2)}Al_{33(13)}C_{16(13)}$, whereas the second phase, light gray, has the composition $Ti_{64(2)}Al_{33(2)}C_{3(1)}$ (Fig. 5*b*). The BSE images reveal the presence of voids in the samples, which makes them unsuitable for hardness measurements.

In agreement with the PXRD data, the microstructures of the samples $Ti_{50}Al_{27}C_{23}$ and $Ti_{50}Al_{19}C_{31}$ revealed the presence of two phases in both samples.

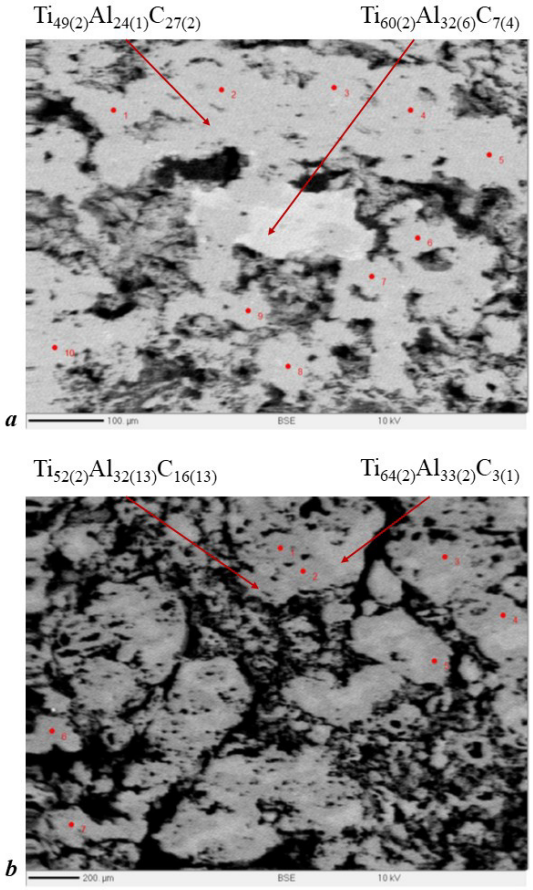


Fig. 5 Microstructures of the (*a*) $Ti_{53}Al_{25}C_{22}$ and (*b*) $Ti_{53}Al_{34}C_{13}$ samples with WDXS compositions of the phases (BSE images).

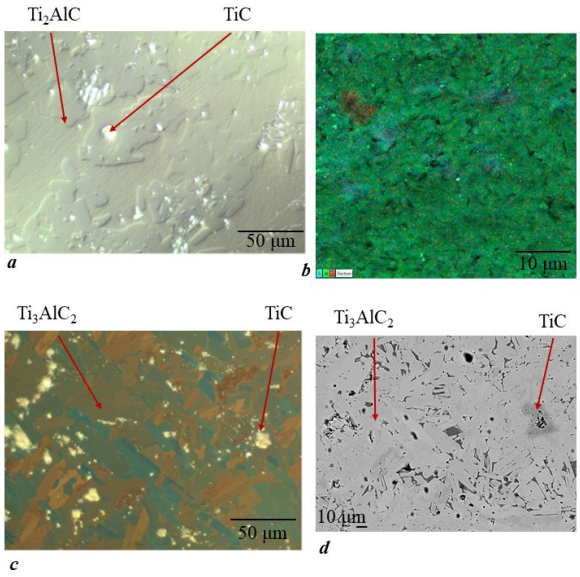


Fig. 6 Microstructure of the samples: $Ti_{50}Al_{27}C_{23}$ – (*a*) optical image in DIC, (*b*) electron map image and $Ti_{50}Al_{19}C_{31}$ – (*c*) optical image in polarized light, (*d*) BSE image.

The sample $Ti_{50}Al_{27}C_{23}$ had as main phase Ti_2AlC, accompanied by TiC containing some Al (Fig. 6*a*,*b*). The composition obtained by EDXS was $Ti_{42.3}Al_{20.4}C_{37.3}$. The sample $Ti_{50}Al_{19}C_{31}$ also contained a TiC-based phase and the title compound Ti_3AlC_2 (Fig. 6*c*,*d*). The composition of the latter was $Ti_{43.5}Al_{25.1}C_{31.4}$.

PXRD data collections for the samples $Ti_{50}Al_{27}C_{23}$ and $Ti_{50}Al_{19}C_{31}$ were used for structure refinements. The compound Ti_2AlC belongs to the structure type Cr_2AlC, and Ti_3AlC_2 to the type Ti_3SiC_2 [9]. The final atomic coordinates and displacement parameters are listed in Table 3 and interatomic distances in Table 4. The structures of Ti_2AlC and Ti_3AlC_2 are characterized by layers of edge-sharing $\underline{C}Ti_6$ octahedra that alternate with layers of Al atoms, which are located at the centers of trigonal prisms. For Ti_2AlC the coordination polyhedron of the Ti atoms is an octahedron, formed by six C atoms ($\underline{Ti}C_6$). The Al atoms have a heteroatomic coordination including six Ti atoms forming a trigonal prism. If also Al–Al contacts are considered, the total coordination number is 12 (Fig. 7). The structure of Ti_3AlC_2 has two sites occupied by Ti atoms. The coordination number of both sites is 6. Six C atoms form an octahedron around the site Ti1 ($\underline{Ti1}C_6$), whereas three C and three Al atoms form a trigonal antiprism (distorted octahedron) around the site Ti2 ($\underline{Ti2}C_3Al_3$). As in Ti_2AlC, the Al atoms have a heteroatomic coordination containing six Ti atoms and six Al atoms, which together form an $\underline{Al}Ti_6Al_6$ polyhedron (Fig. 8).

Table 3 Atomic positions and displacement parameters B_{iso} (Å^2) for Ti_2AlC and Ti_3AlC_2, space group $P6_3/mmc$.

Ti_2AlC						Ti_3AlC_2					
Atom	Wyckoff position	*x*/*a*	*y*/*b*	*z*/*c*	B_{iso}	Atom	Wyckoff position	*x*/*a*	*y*/*b*	*z*/*c*	B_{iso}
Ti	4*f*	⅓	⅔	0.5851(1)	0.71(3)	Ti1	2*a*	0	0	0	1.21(6)
Al	2*c*	⅓	⅔	¼	0.64(8)	Ti2	4*f*	⅓	⅔	0.1275(1)	1.27(4)
C	2*a*	0	0	0	0.7	Al	2*c*	0	0	¼	0.21(1)
						C	4*f*	⅓	⅔	0.5705(3)	0.7

Table 4 Interatomic distances (Å) for Ti_2AlC and Ti_3AlC_2.

Ti_2AlC			Ti_3AlC_2		
Ti	×3C	2.1074(4)	Ti1	×6C	2.240(2)
	×3Al	2.8671(6)		×6Ti2	2.9788(7)
	×3Ti	2.9019(9)		×6Ti1	3.0702(1)
	×6Ti	3.0567(1)	Ti2	×3C	2.047(2)
Al	×6Ti	2.8671(6)		×3Al	2.8549(7)
	×6Al	3.0567(1)		×3Ti1	2.9788(7)
C	×6Ti	2.1074(4)		×6Ti2	3.0702(1)
			Al	×6Ti2	2.8549(7)
				×6Al	3.0702(1)
			C	×3Ti2	2.047(2)
				×3Ti1	2.240(2)

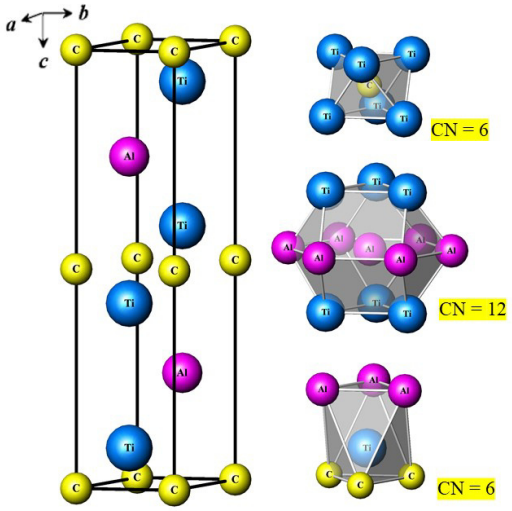


Fig. 7 Unit-cell content of the structure of Ti_2AlC and coordination polyhedra of the atoms.

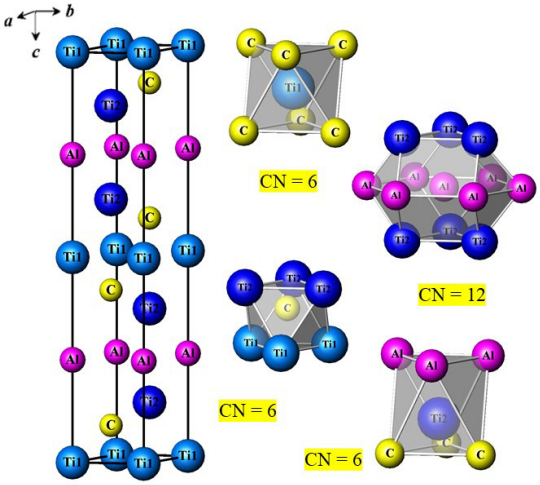


Fig. 8 Unit-cell content of the structure of Ti_3AlC_2 and coordination polyhedra of the atoms.

The density of the MAX phases typically varies between 4 and 6 g·cm^{-3} [1]. The samples with a large amount of the main phase Ti_2AlC or Ti_3AlC_2 have relatively low densities, 4.09 and 4.15 g·cm^{-3}, respectively (Table 5), consistent with the calculated values and literature data [12]. The values are comparable to those of structural ceramics such as Al_2O_3 (4.0 g·cm^{-3}), SiC (3.2 g·cm^{-3}), and Si_3N_4 (3.2 g·cm^{-3}) [1].

The hardness was measured by Vickers method for different loads: 100 g, 300 g, and 400 g (Fig. 9). A laser scanning microscope was used to select planes of grains belonging to the main phase, free of secondary-phase inclusions. The values depended on the applied load. The hardness of the compound Ti_2AlC was within the range 3.4-6.0 GPa, while that of the compound Ti_3AlC_2 was slightly lower, ranging from 3.2 to 3.9 GPa (Table 5).

Table 5 Vickers hardness at different loads and density for three Ti–Al–C samples.

Sample		$Ti_{50}Al_{27}C_{23}$		$Ti_{50}Al_{29}C_{21}$		$Ti_{50}Al_{19}C_{31}$	
		HV	GPa	HV	GPa	HV	GPa
Hardness	100 g	465	4.6	607	6.0	325	3.2
	300 g	393	3.9	344	3.4	398	3.9
	400 g	570	5.6	422	4.1	–	–
Density, $g \cdot cm^{-3}$		4.09		4.09		4.15	

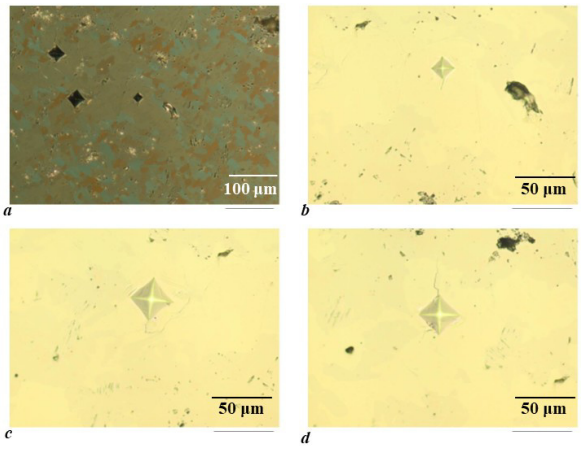


Fig. 9 (*a*) Optical image in polarized light and the SEM images of the sample $Ti_{50}Si_{27}C_{23}$ show the hardness measurement at varying loads: (*b*) 100 g; (*c*) 300 g; (*d*) 400 g.

In addition to the applied load, the direction of grain growth affects the hardness of the samples.

Conclusions

Samples containing MAX phases in the Ti–Al–C system were synthesized by spark plasma sintering (SPS) at different temperatures with the aim to separate the Ti_2AlC and Ti_3AlC_2 phases. According to DTA analysis, the temperatures corresponding to the maximum amount of these compounds are close to each other, differing by approximately 20°C. The highest yields were obtained for samples synthesized at 1300°C and 1350°C for Ti_2AlC and Ti_3AlC_2, respectively.

The unit-cell parameters as obtained from PXRD indicate the absence of a significant homogeneity range. For Ti_2AlC, the following values were found: a = 3.0406(3)-3.0593(4) Å and c = 13.6297(9)-13.660(2) Å, and for Ti_3AlC_2: a = 3.07027(8)-3.0717(3) Å and c = 18.5274(6)-18.558(2) Å.

The MAX phases Ti_2AlC and Ti_3AlC_2 exhibited relatively low densities, 4.09 and 4.15 $g \cdot cm^{-3}$, consistent with previously reported values. The Vickers hardness was in the range 3.2-6.0 GPa, indicating that these materials can be easily machined using conventional mechanical tools.

Acknowledgment

This work was carried out under an EIRENE Grant of the Max Planck Society. The authors thank M. Schmidt for the thermal analysis, U. Burkhardt for the microstructure measurement, R. Cardoso-Gil and Yu. Grin for their support (Max-Planck-Institute for Chemical Physics of Solids).

References

[1] J. Gonzalez-Julian, *J. Am. Ceram Soc.* 104 (2021) 659-690. https://doi.org/10.1063/1.4803700
[2] W. Jeitschko, H. Nowotny, F. Benesovsky, *Mh. Chem.* 331 (1963) 2-6. https://doi.org/10.1007/BF00913068
[3] N.J. Lane, S.C. Vogel, E.N. Caspi, M.W. Barsoum, *J. Appl. Phys.* 113 (2013) 183519 (11 p.). https://doi.org/10.1063/1.4803700
[4] Y. Bai, X. He, Y. Li, C. Zhu, S. Zhang, *J. Mater. Res.* 24 (2009) 2528-2535. https://doi.org/10.1557/jmr.2009.0327
[5] M.A. Pietzka, J.C. Schuster, *J. Phase Equilib.* 15 (1994) 392-400. https://doi.org/10.1007/bf02647559
[6] E. Wu, J. Wang, H. Zhang, Y. Zhou, K. Sun, Y. Xue, *Mater. Lett.* 59 (2005) 2715-2719. https://doi.org/10.1016/j.matlet.2005.03.063
[7] C. Wang, T. Yang, C.L. Tracy, C. Lu, H. Zhang, Y.J. Hu, L. Wang, L. Qi, L. Gu, Q. Huang, J. Zhang, J. Wang, J. Xue, R.C. Ewing, Y. Wang, *Nat. Commun.* 10 (2019) 622 (9 p.). https://doi.org/10.1038/s41467-019-08588-1
[8] H. Zhang, X. Wang, Y. Ma, L. Sun, L. Zheng, Y. Zhou, *J. Adv. Ceram.* 1 (2012) 268-273. https://doi.org/10.1007/s40145-012-0034-9
[9] P. Villars, K. Cenzual (Eds.), *Pearson's Crystal Data: Crystal Structure Database for Inorganic Compounds*, Release 2024/25, ASM International, Materials Park, Ohio, USA.
[10] X. Wang, H. Zhang, L. Zheng, Y. Ma, X. Lu, Y. Sun, Y. Zhou, *J. Am. Ceram. Soc.* 95 (2012) 1508-1510. https://doi.org/10.1111/j.1551-2916.2012.05158.x

[11] M.W. Barsoum, *Solid State Chem.* 28 (2000) 201-281. https://doi.org/10.1016/S0079-6786(00)00006-6
[12] X. Li, X. Xie, J. Gonzalez-Julian, J. Malzbender, R. Yang, *J. Eur. Ceram. Soc.* 40 (2020) 5258-5271. https://doi.org/10.1016/j.jeurceramsoc.2020.07.043
[13] D.B. Lee, T.D. Nguyen, S.W. Park, *J. Alloys Compd.* 469 (2009) 374-379. https://doi.org/10.1016/j.jallcom.2008.01.111
[14] N.V. Tzenov, M.W. Barsoum, *J. Am. Ceram. Soc.* 83 (2000) 825-832. https://doi.org/10.1111/j.1151-2916.2000.tb01281.x
[15] W.B. Zhou, B.C. Mei, J.Q. Zhu, X.L. Hong, *Mater. Lett.* 59 (2005) 131-134. https://doi.org/10.1016/j.matlet.2004.07.052
[16] M.A. Bortnitskaya, E.N. Reshetnyak, A.S. Kuprin, T.A. Prikhana, V.B. Sverdun, I.V. Kolodiy, V.A. Belous, V.G. Marinin, T.B. Serbenyuk, *J. Nano-Electron. Phys.* 13 (2021) 05031 (7 p.). https://doi.org/10.21272/jnep.13(5).05031
[17] R.A. Young (Ed.), *The Rietveld Method*, Oxford University Press, Oxford, United Kingdom, 1995, 298 p.
[18] L. Akselrud, Yu. Grin, *J. Appl. Crystallogr.* 47 (2014) 803-805. https://doi.org/10.1107/S1600576714001058
[19] E. Dowty, *ATOMS. A Computer Program for Displaying Atomic Structures*, Kingsport, TN, USA, 1999.